Astron. Astrophys. 354, 253–260 (2000)

ASTRONOMY AND ASTROPHYSICS

Electron densities, temperatures and ionization rates in two interstellar clouds in front of β Canis Majoris, as revealed by UV absorption lines observed with IMAPS

Edward B. Jenkins[1], **Cécile Gry**[2,3], **and Olivier Dupin**[3]

[1] Princeton University Observatory, Princeton, NJ 08544-1001, USA (ebj@astro.princeton.edu)
[2] ISO Data Center, ESA Astrophysics Division, PO Box 50727, 28080 Madrid, Spain (present address) (cgry@iso.vilspa.esa.es)
[3] Laboratoire d'Astronomie Spatiale, B.P. 8, 13376 Marseille cedex 12, France

Received 7 September 1999 / Accepted 13 December 1999

Abstract. The spectrum of β CMa (Mirzam) between 1000 and 1200Å was recorded at a wavelength resolving power $\lambda/\Delta\lambda \sim 60\,000$ by the Interstellar Medium Absorption Profile Spectrograph (IMAPS) during its orbital flight on the ORFEUS-SPAS II mission in 1996. New information about interstellar absorption lines of C II, C II*, N I and O I from this spectrum are combined with the HST results reported by Dupin & Gry (1998) to arrive at new conclusions about the physical properties of the absorbing gas in front of β CMa. For two prominent velocity components centered at heliocentric velocities of +20.0 and $+30.5\,\mathrm{km\,s^{-1}}$, designated by Dupin & Gry as Components C and D, respectively, we use determinations of $N(\mathrm{C\,II*})/N(\mathrm{C\,II})$ and $N(\mathrm{Mg\,I})/N(\mathrm{Mg\,II})$ to solve for temperatures and electron densities. From our knowledge that oxygen and nitrogen have their ionizations coupled to that of hydrogen through charge exchange reactions, we can derive the hydrogen ionizations by comparing these elements to sulfur, which is likely not to be depleted onto dust grains. For Component C with an approximate column density of neutral and ionized hydrogen $N(\mathrm{H_{total}}) = 6 \times 10^{18}\mathrm{cm^{-2}}$, we find that the neutral fraction $n(\mathrm{H\,I})/n(\mathrm{H_{total}}) = 0.25$, $400 < T < 6500\,\mathrm{K}$, and $0.08 < n(e) < 0.6\,\mathrm{cm^{-3}}$, while for Component D with $N(\mathrm{H_{total}}) = 1.2 \times 10^{19}\mathrm{cm^{-2}}$, we arrive at $n(\mathrm{H\,I})/n(\mathrm{H_{total}}) = 0.035$, $8000 < T < 14\,000\,\mathrm{K}$, and $0.09 < n(e) < 0.2\,\mathrm{cm^{-3}}$. The relatively large ionization fractions of H can arise if the clouds are about 130 pc away from us, so that they are exposed to the strong, ionizing radiation fields from ϵ and β CMa. The presence of Si III indicates the existence of additional gas with even higher levels of ionization.

Key words: ISM: abundances – ISM: atoms, ions – ISM: bubbles – ISM: clouds

1. Introduction

The line of sight toward the B1 II-III star β CMa in the direction (l_{II}, b_{II})=(226.°, −14.°) has raised interest since its first study in the UV from *Copernicus* observations when Gry et al. (1985) showed that it contained very little neutral gas and that a great majority of the material on the line of sight was ionized. Indeed for a distance now set to 153 pc by Hipparcos measurements, Gry et al (1985) determined that N(H I) was somewhere within the range $1 - 2.2\ 10^{18}\mathrm{cm^{-2}}$ based on the interstellar Lyβ absorption profile in the spectrum of β CMa recorded by *Copernicus*, and showed that the total (neutral and ionized) hydrogen column density was ten times higher using the combined abundances of S II and S III compared to that of H I multiplied by the cosmic ratio of S to H. EUVE observations independently confirmed both findings. Cassinelli et al. (1996) found N(H I)=$2.0 \pm 0.2\ 10^{18}\mathrm{cm^{-2}}$ by fitting the Lyman limit absorption in the EUV spectrum of the star. Evidence for ionization comes from the lower limits for the continuum absorption by He I in the spectrum of β CMa which indicate that $N(\mathrm{He\,I}) > 6.\ 10^{17}\mathrm{cm^{-2}}$ (Aufdenberg et al. 1999) or $> 1.4\ 10^{18}\mathrm{cm^{-2}}$ (Cassinelli et al. 1996), depending on assumptions about the drop in stellar flux across the He I ionization edge. The fact that $N(\mathrm{He\,I}) \gg 0.1N(\mathrm{H\,I})$ indicates that a substantial fraction of the hydrogen toward β CMa is ionized.

The weak presence of H I gas in this region of the sky is particularly evident in the neighbouring line of sight toward ϵ CMa ($l_{II} = 239.°8$, $b_{II} = -11.°3$) where the Lyman limit absorption is even lower (Cassinelli et al. 1995). Gry et al. (1995) found a H I column density upper limit of $5\ 10^{17}$ and showed furthermore that almost all the neutral gas is very close to the Sun, distributed in two small components which are also detected with similar column densities in the line of sight to Sirius 2.7 pc away (Lallement et al. 1994). Because of the scarcity of H I in this region, ϵ CMa and β CMa are the two strongest sources of EUV radiation, and the two stars, especially ϵ CMa, dominate the H-ionization field close to the Sun (Vallerga & Welsh 1995; Vallerga 1997). The conditions along these lines of sight, especially their ionization structure, strongly influence the nature and ionization of the local interstellar matter. Yet even with this in mind, we find that the ionization of the local ISM is not very well understood. For instance, with the radiation from ϵ and β CMa plus other easily identifiable sources of ionizing ra-

Send offprint requests to: C. Gry

Table 1. Interstellar absorption lines detected in the β CMa IMAPS data.

Element	λ	f
C II	1036.337	$1.23\ 10^{-1}$
C II*	1037.018	$1.23\ 10^{-1}$
N I	1134.165	$1.34\ 10^{-2}$
	1134.415	$2.68\ 10^{-2}$
	1134.980	$4.02\ 10^{-2}$
N II	1083.990	$1.03\ 10^{-1}$
O I	1039.230	$9.20\ 10^{-3}$
Si II	1190.416	$2.50\ 10^{-1}$
	1193.290	$4.99\ 10^{-1}$

diation, it is difficult to reconcile the fact that helium appears to be more ionized than hydrogen, as revealed by evidence from the EUVE spectra of several white dwarfs (Dupuis et al. 1995).

High resolution observations with GHRS on board HST allowed Dupin & Gry (1998) to show that the bulk of the gas in the β CMa sight-line is distributed in two main components separated by 10 km/s, which are warm, only slightly depleted and both mostly ionized. However the analysis of the ionization processes was hampered by the fact that several species and especially the neutral species had been observed with a limited resolution of about 20 000 which did not allow for a clear separation of the two components. The relative distribution of matter in the two components therefore had uncertainties that allowed only lower limits to the ionization fractions to be derived.

Here we present new observations performed with the Interstellar Medium Absorption Profile Spectrograph (IMAPS) (Jenkins, et al. 1996), with the aim of gaining further insights on the ionization structure and various physical processes in the local interstellar medium. The higher resolution of 60 000 provided by IMAPS allowed us to resolve the absorptions of the two main components which in turn permitted the derivations of ionization fractions in each cloud. We also determined the clouds' electron densities using the observation of C II*, which ultimately led to new insights on the ionization process.

2. Observations and data reduction

The observations were carried out by IMAPS when it was operated on the ORFEUS-SPAS II mission that flew in late 1996 (Hurwitz et al. 1998). IMAPS is an objective-grating echelle spectrograph that was designed to record the spectra of bright, early-type stars over the wavelengths from ~ 950 Å to ~ 1150 Å with a high spectral resolution. For more details on the instrument see Jenkins et al. (1988, 1996).

The spectra were extracted from the echelle spectral images using special procedures developed by one of us (EBJ) and his collaborators on the IMAPS investigation team. A zero point in the wavelength calibration was made by measuring the O I* and O I** telluric lines detected at 1040.943 Å and 1041.688 Å. Table 1 presents the interstellar lines detected in the data, with wavelengths and f-values taken from Morton (1991).

3. Analysis

The structure of velocity components in the sight-line toward β CMa has already been determined by the analysis of GHRS HST data (Dupin & Gry 1998): four components were detected, two of which (designated as Components C and D) were strongly dominant, and the remaining two (A and B) showed up only for the strongest lines. In the study conducted by Dupin & Gry (1998), only the lines between 1800 Å and 3000 Å (Fe II, Mg II, Mg I and Si II lines) were observed at a resolution $\lambda/\Delta\lambda \sim 80\,000$. Because of the failure of the Echelle A grating at the time of the observations, all the species that had lines between 1150 Å and 1800 Å were observed at medium resolution ($\sim 20\,000$). With a resolution of $\sim 60\,000$, the IMAPS spectrograph now allows us to analyse lines of some important species like N I and O I at a resolution comparable to that of the GHRS Echelle data. As a consequence, we can resolve partially clouds C and D which are separated by only $10\,\mathrm{km\,s^{-1}}$. To facilitate a comparison between the IMAPS data and the HST data that were presented by Dupin & Gry (1998), we interpreted the column density vs. velocity profiles in terms of the components defined by them. However, the data are not precise enough to rule out other, slightly different combinations of components that could produce fits that are just as acceptable.

The relative velocities between the four clouds are precisely known from the Dupin & Gry (1998) study. The heliocentric radial velocities found in our study are larger than those of Dupin & Gry (1998) by about $5.5\,\mathrm{km\,s^{-1}}$. This difference is larger than the stated error for the GHRS velocity zero points, but we favor the velocities from the IMAPS data because we could use the telluric absorption lines as a reference. The velocity of C II* is especially good since it is very close to the O I** line at 1041.688Å in the spectral format of the IMAPS echelle and cross disperser gratings. The velocity dispersions b for C II, N I and O I in Components C and D are not well determined, since some blurring of the lines is caused by the instrument. However, they should be constrained by b(Mg II) on the low end and the measured widths on the upper end. Thus, the principal free parameters are the column densities of various species in cloud C and cloud D. For the strong lines of N I and O I we see some evidence for the presence of Component B, and we can place upper limits for the strength of A.

The principal source of uncertainty for the column densities is the determination of the background intensity caused by scattered light from the echelle and cross disperser gratings in IMAPS. As is evident from Jenkins et al. (1996 – see their Fig. 12) there is some overlap of energy from adjacent echelle orders, precluding the use of the interorder regions for measuring the background levels. We could determine the overall behavior of the scattered light by examining the trends for the bottoms of strong stellar absorption features. For the background level below the line of C II* at 1037.018Å, we could use the nearby, saturated absorption from interstellar C II at 1036.337Å.

Fig. 1 shows the features recorded by IMAPS after they were normalized to the stellar continuum. Overplotted on these data are the predicted absorption profiles for the column densities

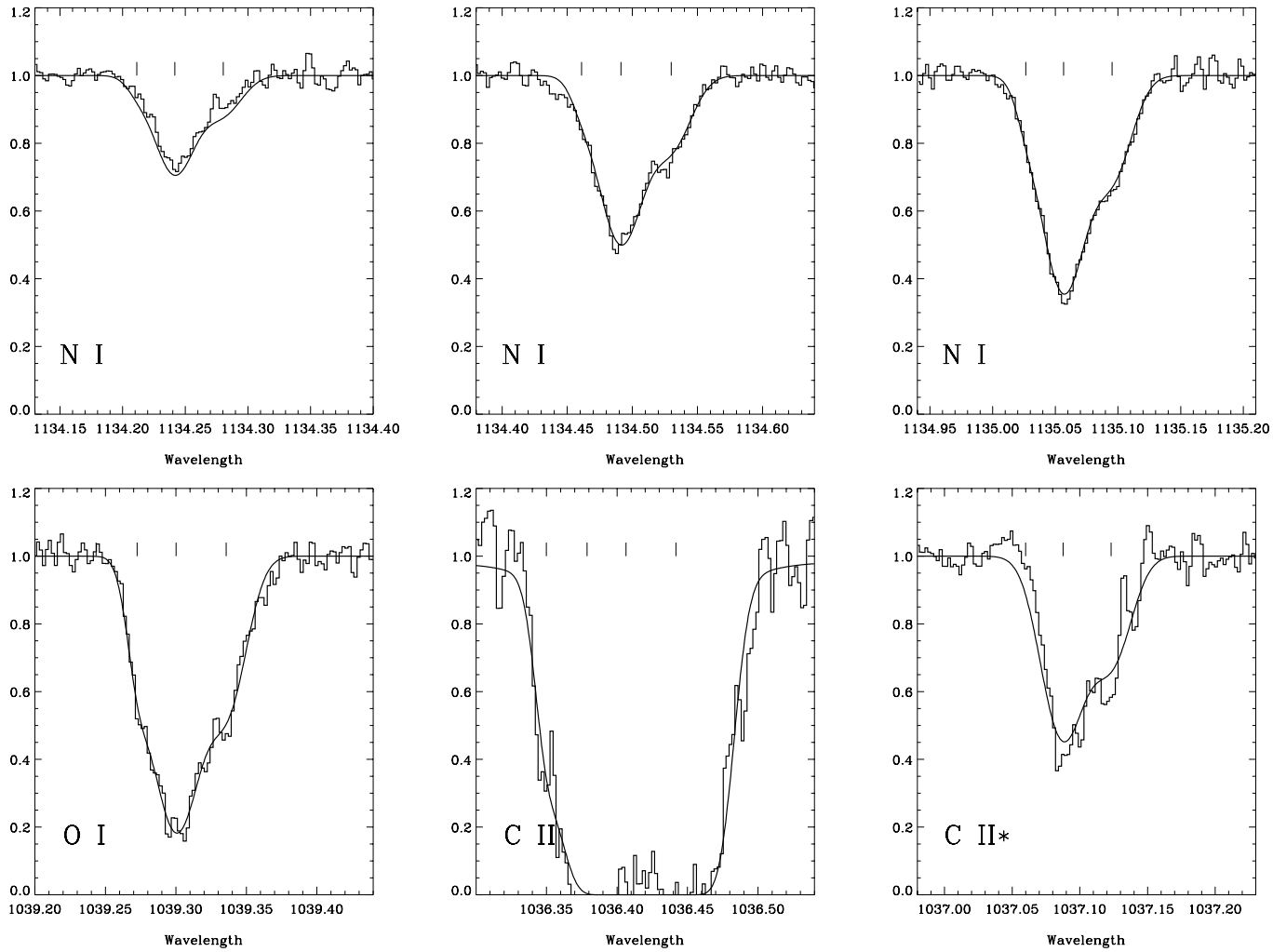

Fig. 1. Interstellar lines observed with IMAPS. The histogram-style tracings represent the recorded data after normalization to the stellar continuum, and the smooth lines show the fits obtained from our analysis. The tick marks above the absorption features denote (left to right) the positions of the velocity Components B, C and D identified in the text, except for C II which shows Component A (far left) in addition to the others.

Table 2. Velocities and column densities for various species toward β CMa.

Component	$v_\odot$ (km s^{-1})	N(C II) (cm^{-2})	N(C II*) (cm^{-2})	N(N I) (cm^{-2})	N(O I) (cm^{-2})
A	3.0	$\sim 1.7\ 10^{13}$	$\leq 1.\ 10^{11}$	$\leq 1.\ 10^{11}$	$\leq 1.\ 10^{11}$
B.....	11.0	$\sim 2\ 10^{15}$	$\leq 1.\ 10^{11}$	$\leq 4.\ 10^{12}$	$7.5 \pm 2.5\ 10^{13}$
C.....	20.0	saturated	$2.4 \pm 0.1\ 10^{13}$	$9.6 \pm 0.4\ 10^{13}$	$7.6 \pm 0.4\ 10^{14}$
D	30.5	saturated	$1.2 \pm 0.2\ 10^{13}$	$2.7 \pm 0.3\ 10^{13}$	$2.2 \pm 0.2\ 10^{14}$

and central velocities given in Table 2. Selected results for Components C and D derived by Dupin & Gry (1998) are listed in Table 3, as an aid to following the interpretations that we present in Sect. 4. We made no attempt to measure the Si II lines listed in Table 1, since they were saturated and not nearly as useful as the transition at 1808 Å observed by Dupin & Gry (1998). Conversely, our N I lines are not saturated, but the weakest member of the 1200 Å multiplet observed by Dupin & Gry had a central optical depth $\tau_0 = 1.7$ for Component C [derived from our N(N I) and their b value]. The lack of saturation and higher resolution for the IMAPS recordings of N I absorption lead to our preferring the values derived here to those of Dupin & Gry, even though there is some uncertainty in the IMAPS background level.

The O I transition at 1302 Å observed by Dupin & Gry was hopelessly saturated, which led to their only being able to express a lower limit for N(O I). Fig. 1 shows that the IMAPS recording of the much weaker transition at 1039 Å shows a

Table 3. Selected results from Dupin & Gry's (1998) study of β CMa.

Species	Comp. C	Comp. D
N(S II) (cm^{-2})	$1.1 \pm 0.4\ 10^{14}$	$2.3 \pm 0.5\ 10^{14}$
N(Si II)	$5.8 \pm 0.5\ 10^{13}$	$7.5 \pm 0.3\ 10^{13}$
N(Si III).....	$\leq 5\ 10^{12}$	$(1.5 - 10)10^{14}$
N(Mg I).....	$8.0 \pm 0.6\ 10^{10}$	$2.5 \pm 0.3\ 10^{11}$
N(Mg II).....	$3.1 \pm 0.6\ 10^{13}$	$5.9 \pm 0.8\ 10^{13}$
N(Fe II).....	$1.2 \pm 0.1\ 10^{13}$	$1.0 \pm 0.1\ 10^{13}$

fairly strong saturation. If there are narrow, unresolved subcomponents within Component C that are far more saturated than what we see in the apparent residual intensity of the line, our listed column density may be below the true value. In principle, one could sense the presence of such components by observing that the N I absorptions do not grow as fast as their increases in transition strengths. However the lines that we observed here are too weak to show this effect well. Nevertheless, it is interesting to note that by observing the strong multiplet of N I at 1200 Å Dupin & Gry (1998) found $N(\mathrm{N\,I} = 8.1 \pm 0.8\ 10^{13}\mathrm{cm}^{-2}$ for Component C (including the hidden local clouds)[1], which is only 0.84 times the value that we obtained (see Table 2). (Our and their results for Component D agree however.) Thus, when lines reach a strength similar to that of the O I line at 1039 Å, the column densities might be understated by a factor of about 0.84.

4. Interpretation

4.1. Radial velocities

As noted earlier, there is a systematic offset between the velocities reported here and those given by Dupin & Gry (1988). Our new velocity for Component C at $20\,\mathrm{km\,s}^{-1}$ makes it consistent with that of gas in the Local Interstellar Cloud (LIC), moving at a velocity of $26\,\mathrm{km\,s}^{-1}$ towards the direction $l = 186^\circ$ and $b = -16^\circ$ (Lallement & Bertin 1992), whereas Dupin & Gry felt that the LIC was buried in the gap between Components C and D. However, there are two important problems for identifying the origin of Component C with the LIC. First, the column densities of Mg II and Fe II in Component C (see Table 3) are considerably larger than $N(\mathrm{Mg\,II}) = 1.65\ 10^{12}\mathrm{cm}^{-2}$ and $N(\mathrm{Fe\,II}) = 8.5\ 10^{11}\mathrm{cm}^{-2}$ found in the LIC component at $18.8\,\mathrm{km\,s}^{-1}$ in the spectrum of α CMa (Lallement, et al. 1994) which is only 5.5° away in the sky, and than $N(\mathrm{Mg\,II}) = 3.0\ 10^{12}\mathrm{cm}^{-2}$ and $N(\mathrm{Fe\,II}) = 1.35\ 10^{12}\mathrm{cm}^{-2}$ found in the LIC component at $17\,\mathrm{km\,s}^{-1}$ in the spectrum of ϵ CMa (Gry et al. 1995), 17° away in the sky. Also, $N(\mathrm{H\,I}) = 5\ 10^{17}\mathrm{cm}^{-2}$ in front of α CMa (Holberg et al. 1998) is only about a third as large as the H I column density that we identify with Component C [$N(\mathrm{H\,I}) = 1.6\ 10^{18}\mathrm{cm}^{-2}$, taken from N(N I) and N(O I) after correcting for depletion – see Sect. 4.2 below.] Even though α CMa is only 2.6 pc away, it seems to lie beyond the boundary of the LIC because Lallement et al. (1994) detected another (somewhat weaker) component at $v = 13\,\mathrm{km\,s}^{-1}$. Second, we show in Sect. 4.5 that the ionizing radiation field that is needed to sustain the ionization is considerably higher than that found for the local vicinity. Thus, the agreement of velocity of Component C with that of the LIC is probably just coincidental.

4.2. Column densities, depletions, and ionization fractions

We define a depletion factor $\delta(X)$ of an element X in terms of its column density $N(X)$, relative to that of hydrogen $N(\mathrm{H})$, by the expression

$$\delta(X) = \left(\frac{N(X)}{N(\mathrm{H})}\right)\ \left(\frac{\mathrm{H}}{X}\right)_{\mathrm{cosmic}} \quad (1)$$

where $(\mathrm{H}/X)_{\mathrm{cosmic}}$ is the cosmic abundance ratio.[2] For such a depletion to be meaningful in any given circumstance, one must account for differences in the observed ionization stage(s) of element X relative to that adopted for H (either H I or $\mathrm{H}_{\mathrm{total}}$). We address this consideration in the cases that follow, starting with the simplest ones involving the elements nitrogen, oxygen and sulphur.

The relative ionizations of N I and O I are closely coupled to that of H I through the large charge exchange reaction rates that arise from their nearly equal ionization potentials (Field & Steigman 1971; Butler & Dalgarno 1979). In the diffuse interstellar medium, these two elements are only mildly depleted below their cosmic abundances relative to hydrogen (Hibbert et al. 1985; Cardelli et al. 1991a,b; Meyer et al. 1994, 1997, 1998), so they can serve as reasonably good indicators for H I in a partially ionized region. Sulphur is another element that has little or no depletion onto dust grains, but its second ionization potential is very high (23 eV). If the photoionization rate arising from photons with $E > 23$ eV is not very large, we expect that S II should be a good indicator of the total hydrogen in the line of sight, both in the neutral and ionized forms. In essence, for N, O and S we can make use of our general understanding of their depletions to arrive at conclusions on the relative ionization of hydrogen.

With our ability to identify how much of the absorptions by N I and O I can be assigned to Components C and D, we can differentiate between the relative fractions of H in neutral form in each case, after making comparisons with Dupin & Gry's (1998) values for S II in these same components. In doing this, we invoke two assumptions about the depletions: (1) the depletions of N and O onto dust grains are the same for Components C and D, and (2) S is undepleted. Assumption (1) seems reasonable in the light of evidence presented by Meyer et al. (1997, 1998) and (2) seems justified from the evidence summarized by Savage & Sembach (1996) and Fitzpatrick & Spitzer (1997). If either of these assumptions is not quite correct, small errors

[1] Note that in Dupin & Gry Table 2, the listed column densities for Component C had a contribution from the LIC and the other local cloud detected in both α CMa and ϵ CMa sightlines subtracted off. This contribution is negligible for all species but O I and N I for which it represents about 25% of the total absorption in Component C.

[2] Throughout this paper, we use the cosmic abundances of Anders & Grevesse (1989)

in our conclusions may arise. However, they are probably not much worse than the uncertainty in identifying the relative contributions of Components C and D in the low resolution spectra of the S II features.

For nitrogen, we obtain a general depletion factor $\delta(\mathrm{N}) = 0.55$ through Eq. (1) by taking $N(\mathrm{N\,I})_{\mathrm{C+D}}$, dividing it by $N(\mathrm{H\,I}) = 2.\ 10^{18}\mathrm{cm}^{-2}$, and then multiplying the result by the cosmic ratio of H to N. The same analysis for O leads to $\delta(\mathrm{O}) = 0.58$. These values, incidentally, are not much different from those shown by Meyer et al. (1997, 1998). We now estimate the hydrogen neutral fractions in each component from the expression (for the case of N I)

$$n(\mathrm{H\,I})/n(\mathrm{H_{total}}) = \left(\frac{\mathrm{S}}{\mathrm{N}}\right)_{\mathrm{cosmic}} \frac{N(\mathrm{N\,I})}{\delta(\mathrm{N})N(\mathrm{S\,II})} \quad (2)$$

and likewise for O I. For both N I and O I, we obtain $n(\mathrm{H\,I})/n(\mathrm{H_{total}}) = 0.25$ for Component C and 0.035 for Component D.

The high column density of Si III identified with Component D by Dupin & Gry (1998) presents a special problem (see Table 3). The rate constant for charge exchange between doubly ionized Si and neutral H is about $3.0\ 10^{-9}\mathrm{cm}^3\,\mathrm{s}^{-1}$ at the temperatures of interest to us (Gargaud, et al. 1982). From the electron density derived later in Sect. 4.3 and $n(\mathrm{H\,I})/n(\mathrm{H_{total}})$ for Component D, we find that $n(\mathrm{H\,I}) \sim 0.005\,\mathrm{cm}^{-3}$ (for an applicable temperature that we derive in Sect. 4.4). This density times the charge exchange rate constant is considerably larger than the expected ionization rate $\Gamma(\mathrm{Si\,II}) = 5.\ 10^{-14}\mathrm{s}^{-1}$ that we infer from the hydrogen ionization and the shapes of the EUV spectra of ϵ and β CMa (Vallerga & Welsh 1995; Aufdenberg et al. 1999) which should dominate the photoionizing radiation field. It is hard to reconcile this inequality with Dupin & Gry's finding that $N(\mathrm{Si\,III})/N(\mathrm{Si\,II}) \geq 2$ for Component D. We propose that this contradiction can be overcome by having the Si III exclusively within a different part of the region, perhaps one that is much closer to some ionizing source or, alternatively, within the cloud's conduction/evaporation front at an interface with gaseous material at a much higher temperature. There is empirical evidence that the association of Si III with lower ionization stages is not unusual. For instance, Cowie, et al. (1979) found that the velocity endpoints of O VI, Si III, and N II features were mutually correlated, and they used this evidence to suggest that the interfaces between cool and hot gas were conspicuous in the interstellar absorption lines.

In sections that follow, we will ignore the existence of the Si III-bearing region and propose that the contradiction that we have noted justifies our regarding it as unrelated to the gas that holds most of the lower ionization states.

4.3. Electron densities from N(C II)/N(C II)*

The relative populations of the fine-structure states of C II are governed by the balance between collisions and the radiative decay of the upper level. If electrons are the dominant projectiles for excitation and de-excitation, the rate coefficient for de-excitations is

$$\gamma_{2,1} = \frac{8.63\ 10^{-6}\Omega_{1,2}}{g_2 T^{0.5}}\mathrm{cm}^3\mathrm{s}^{-1} \quad (3)$$

(Spitzer 1978, p. 73), with the reverse rate given by detailed balancing, $\gamma_{1,2} = (g_2/g_1)\exp(-E_{1,2}/kT)\gamma_{2,1}$. The statistical weights of the levels are $g_1 = 2$ and $g_2 = 4$, and the temperature equivalent for the difference in energy levels $E_{1,2}/k = 94.9$K. Thus we find that the condition for equilibrium,

$$n(e)\gamma_{1,2}n(\mathrm{C\,II}) = [n(e)\gamma_{2,1} + A_{2,1}]n(\mathrm{C\,II*}) \quad (4)$$

will lead to an equation for the electron density

$$n(e) = \frac{g_2 A_{2,1} T^{0.5}\left[\frac{n(\mathrm{C\,II*})}{n(\mathrm{C\,II})}\right]}{8.63\ 10^{-6}\Omega_{1,2}\left\{\left(\frac{g_2}{g_1}\right)\exp\left(\frac{-E_{1,2}}{kT}\right) - \left[\frac{n(\mathrm{C\,II*})}{n(\mathrm{C\,II})}\right]\right\}} \quad (5)$$

where the radiative decay probability for the upper level is $A_{2,1} = 2.29\ 10^{-6}\mathrm{s}^{-1}$ (Nussbaumer & Storey 1981), and the collision strength $\Omega_{1,2} = 2.81$ (Hayes & Nussbaumer 1984). Optical pumping of the C II fine structure levels is unlikely to happen under the circumstances where there is a very high optical depth in the line (Sarazin, et al. 1979). Also, the density of pumping radiation must be very large – even larger than the elevated levels considered later in Sect. 4.5. Finally, unacceptably high values for $n(\mathrm{H\,I})$ would be needed for collisions by neutrals to have any importance (Keenan et al. 1986).

As is clear from Fig. 1, the C II feature at 1036 Å is far too saturated to allow a determination of $N(\mathrm{C\,II})$ for either Components C or D. Thus, our determination of the column densities must be indirect. A good surrogate for carbon is sulphur. Our repeat of calculations of the type done by Sofia & Jenkins (1998) indicate that in partially ionized gases these two elements have about the same fraction of atoms elevated to higher (unseen) stages of ionization for a wide range of conditions. The depletion of carbon atoms in dense clouds is typically $\delta(\mathrm{C}) = 0.39$ (Cardelli et al. 1993, 1996; Sofia et al. 1998), and, learning from the example of τ CMa (Sofia et al. 1997), this level of depletion seems to hold also for low density lines of sight. On the assumption that carbon toward β CMa is depleted by this factor and there is no depletion of sulphur, we can arrive at $N(\mathrm{C\,II})$ from the product $(\mathrm{C/S})_{\mathrm{cosmic}}\delta(\mathrm{C})N(\mathrm{S\,II})$. Doing so gives us the values $N(\mathrm{C\,II}) = 8.3\ 10^{14}\mathrm{cm}^{-2}$ for Component C and $1.7\ 10^{15}\mathrm{cm}^{-2}$ for Component D, leading to $N(\mathrm{C\,II*})/N(\mathrm{C\,II}) = 0.029^{+0.020}_{-0.012}$ and $0.0071^{+0.0034}_{-0.0023}$ for Components C and D, respectively.

Before we can derive values for $n(e)$ from Eq. (5), we must determine T. To do this, we rely on another method for measuring $n(e)$, but one that has a different temperature dependence. The balance between the ionization of Mg I and the recombination of Mg II is a fundamentally different process from that which governs the fine-structure equilibrium of C II, but both are driven by the value for $n(e)$. In the next section (Sect. 4.4), we shall make use of the difference to constrain other free parameter, the temperature T.

4.4. Electron densities from Mg I/Mg II

The equation for the equilibrium of the lowest 2 ionization levels of Mg is given by

$$\left[\Gamma(\mathrm{Mg\,I}) + C(\mathrm{Mg\,II})n(H^+)\right]n(\mathrm{Mg\,I}) = \alpha(\mathrm{Mg\,I})n(e)n(\mathrm{Mg\,II}) \quad (6)$$

For the charge exchange rate $C(\mathrm{Mg\,II})$ that applies to the reaction Mg I + $H^+ \rightarrow$ Mg II + H, we used the analytical approximation $C(\mathrm{Mg\,II}) = 1.74\ 10^{-9} \exp(-2.21\ 10^4/T)$ derived by Allan, et al. (1988). Collisional ionization of Mg I is negligible at the temperatures of interest in this study. We computed $\Gamma(\mathrm{Mg\,I})$ at the position of the Sun using mean of the stellar radiation fields estimated by Jura (1974) $\lambda F_\lambda = 3.0\ 10^{-3}\mathrm{erg\ cm^{-2}s^{-1}}$ and Mathis, et al. (1983) $\lambda F_\lambda = 2.5\ 10^{-3}\mathrm{erg\ cm^{-2}s^{-1}}$, multiplied by the photoionization cross section given by Verner et al. (1996), to arrive at $\Gamma(\mathrm{Mg\,I}) = 6.1\ 10^{-11}\mathrm{s^{-1}}$. (However, this number increases to $9.5\ 10^{-11}\mathrm{s^{-1}}$ when we consider locations closer to ϵ and β CMa at a later stage of the analysis.) For $\alpha(\mathrm{Mg\,I})$ we used the radiative and dielectronic recombination rates given by Shull & van Steenberg (1982), supplemented by the additional contributions from low-lying resonance states computed by Nussbaumer & Storey (1986).

It is immediately evident that the Echelle B observations of Mg I and Mg II by Dupin & Gry (1998) both show an excellent signal-to-noise ratio, a smooth stellar continuum flux, and absorption features that are reasonably well resolved. Nevertheless, there is a difference between the two. On the one hand, the 2853 Å feature of Mg I represents an absorption that is unsaturated and thus straightforward to analyze. On the other hand, the two features of Mg II (2796 and 2803 Å) were heavily saturated, which leads to a large uncertainty in $N(\mathrm{Mg\,II})$. Even though Dupin & Gry could use the well-determined b value for Mg I to help in the interpretation of the Mg II features, the error in N(Mg II) is still significant (see Table 3). We will use here a less direct method of deriving N(Mg II) from similar but more accurately determined species, along with an application of some empirical relationships for interstellar depletions, that will ultimately lead to a completely independent estimate for N(Mg II).

As with C and S discussed in Sect. 4.3, Mg and Si are a good pair of elements that have very similar photoionization properties (although the rate coefficients for charge exchange of their doubly ionized forms with neutral hydrogen are very different – see below). Fitzpatrick (1997) shows a general relationship between the logarithms of the interstellar depletions of Mg and Si. If we assume that S is generally undepleted, we can substitute it for H and then derive the quantity $\log\delta(\mathrm{Mg})$ from our observed $\log\delta(\mathrm{Si})$ and his best fit to the trend $\log\delta(\mathrm{Mg}) = 0.82\log\delta(\mathrm{Si}) - 0.17$ dex. When we do this, we find that $\log\delta(\mathrm{Mg}) = -0.63$ dex for Component C and -0.80 dex for Component D. Products of these derived δ's, the S II column densities, and the cosmic values for Mg relative to S give $N(\mathrm{Mg\,II}) = 5.4\ 10^{13}\mathrm{cm^{-2}}$ and $7.6\ 10^{13}\mathrm{cm^{-2}}$ for Components C and D, respectively. A moderate adjustment in $N(\mathrm{Mg\,II})$ for Component D must be made to account for the fact that about 24% of the Mg is probably in the doubly ionized form, while the fractional amount of Si II is much lower because it has a significantly larger rate coefficient for recombining via charge exchange with neutral hydrogen. This conclusion was derived quantitatively after making preliminary calculations of the ionization balance, as described later in Sect. 4.5. No such correction is needed for Component C. The estimate we made here for $N(\mathrm{Mg\,II})$ for Component C is somewhat larger than the one given in Table 3 – however is marginally consistent with it when the error of 0.16 dex attached to our present method is considered– while our (adjusted) value of $N(\mathrm{Mg\,II}) = 5.8\ 10^{13}\mathrm{cm^{-2}}$ is remarkably close to the value derived by Dupin & Gry. Finally, we arrive at $N(\mathrm{Mg\,I})/N(\mathrm{Mg\,II})$ equal to $0.0015^{+0.0007}_{-0.0005}$ for Component C and $0.0043^{+0.0020}_{-0.0013}$ for Component D. Note that while Dupin & Gry's values for N(S II) have large estimated relative errors (36%, 22%), such errors have a very weak influence in the conclusions because the slope of the empirical relationship between $\log\delta(\mathrm{Mg})$ and $\log\delta(\mathrm{Si})$ is not much different than 1.0. The same applies to errors in the assumption that $\log\delta(\mathrm{S}) = 0.0$ dex.

As a check that the depletions toward β CMa are not out of the ordinary, we carried out a similar exercise, comparing the measured $\log\delta(\mathrm{Fe}) = (-1.20,\ -1.60)$ dex and their respective $\log\delta(\mathrm{Si}) = (-0.56,\ -0.77)$ dex for consistency with the trend shown by Fitzpatrick (1996). Both cases fell within the body of points that defined this trend.

The curved bands in Fig. 2 show, as a function of temperature T, the expected outcomes for $\log N(\mathrm{Mg\,I}) - \log N(\mathrm{Mg\,II})$ found by solving the ionization equilibrium equation (Eq. 6) with the values of $n(e)$ obtained from Eq. 5 and the measured values of N(C II*)/N(C II) given in Sect. 4.3. From the intersections of these curves with the logarithms of the observed $N(\mathrm{Mg\,I})/N(\mathrm{Mg\,II})$ presented above (straight, horizontal bands in the figure), we find that $400 < T < 6500$ K for Component C and $8000 < T < 14\,000$ K for Component D. To compute the upper limits for $n(e)$, we evaluate Eq. (5) with the upper limit for $N(\mathrm{C\,II*})/N(\mathrm{C\,II})$ at the higest temperature that is consistent with this upper limit (*not* the highest temperature allowed in general). For the lower limits, we take the lowest permissible $N(\mathrm{C\,II*})/N(\mathrm{C\,II})$ and apply it to Eq. (5) with the lowest temperature. These conditions for the limits are shown by solid dots in Fig. 2. For Component C we find that $0.08 < n(e) < 0.6\,\mathrm{cm^{-3}}$, and for Component D we arrive at $0.09 < n(e) < 0.2\,\mathrm{cm^{-3}}$. (While our lower limit for $n(e)$ for Component C is formally allowed, the real value of $n(e)$ is probably much closer to the upper limit because the temperature of the gas is probably much higher than 400 K.) These represent the worst possible extremes in $n(e)$ permitted by the data.

4.5. Ionizing radiation

Shortward of the Lyman limit, the general ionizing radiation field near the Sun is dominated by the output of ϵ and β CMa supplemented by many nearby white dwarf stars, cataclysmic variables, and the line emission from some late-type stars (Vallerga 1997). In addition to stellar sources, some diffuse energetic

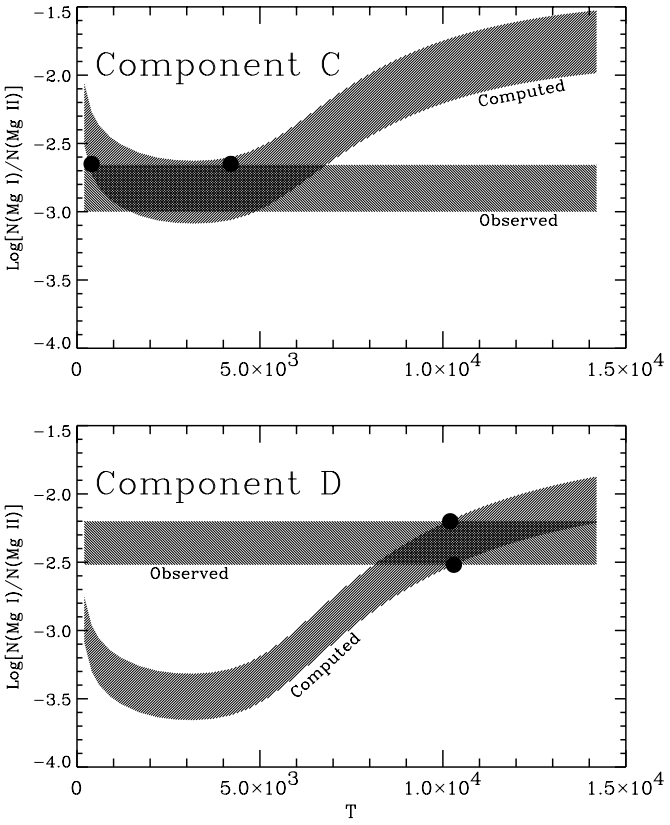

Fig. 2. Predictions for the logarithms of $N(\mathrm{Mg\,I})/N(\mathrm{Mg\,II})$ as a function of temperature T (curved, shaded bands), computed from Eq. 6 using electron densities $n(e)$ derived from the measurements of $N(\mathrm{C\,II*})/N(\mathrm{C\,II})$ applied to Eq. 5. The widths of these bands indicate the ranges that are allowed by our estimated errors. The shaded, straight, horizontal bands indicate the observed values (and their uncertainties) for $\log[N(\mathrm{Mg\,I})/N(\mathrm{Mg\,II})]$. In each case, the overlaps of the straight and curved bands indicate the temperature ranges that are consistent with both the $N(\mathrm{C\,II*})/N(\mathrm{C\,II})$ and $N(\mathrm{Mg\,I})/N(\mathrm{Mg\,II})$ results. Positions on the diagram that represent the worst extremes in $n(e)$ are indicated by solid dots; see the text for details.

radiation from the hot gas that surrounds the LIC may contribute additional ionization (Cheng & Bruhweiler 1990). The intensity of this diffuse radiation is rather uncertain: Jelinsky et al. (1995) have observations that place a meaningful upper limit for this radiation if it produces spectral features in agreement with some specific predictions of hot-gas emission models.

If we calculate the hydrogen ionization produced by Vallerga's (1997) composite EUV stellar radiation field, supplemented by Cheng & Bruhweiler's (1990) hot gas radiation attenuated by absorption from a hydrogen column $N(\mathrm{H\,I}) = 2\ 10^{17}\mathrm{cm}^{-2}$, we find that the neutral fraction of hydrogen is 0.89 and 0.47, for Components C and D, respectively, if we require that $n(e) = 0.31\,\mathrm{cm}^{-3}$ and $0.13\,\mathrm{cm}^{-3}$ as we found from the analysis of $N(\mathrm{C\,II*})/N(\mathrm{C\,II})$ and $N(\mathrm{Mg\,I})/N(\mathrm{Mg\,II})$ in Sects. 4.3 and 4.4. This is clearly inconsistent with our finding $N(\mathrm{H\,I})/N(\mathrm{H_{total}}) = 0.25$ and 0.035 for the two components in Sect. 4.2. The model calculations followed the scheme outlined by Sofia & Jenkins (1998) that included the ionization of helium and allowed for the extra electrons coming from He. (In contrast to the LIC, where helium ionization is important, the models indicated that the high values of $n(e)$ effectively suppressed the ionization of helium.)

To overcome the fact that the predicted ionization of H is less than observed, we must find additional sources of ionization. One possibility is that there is vestigial ionization left over from a previous event that heated the gas and collisionally ionized it (Lyu & Bruhweiler 1996), such as the passage of a shock front in less a few times 10^5yr ago. If this were the case, it would be difficult to explain why the gas is not moving at a substantial velocity. Another tactic is to propose that most of the gas that we see is rather close to ϵ and β CMa, where the hydrogen (and helium) ionization rates must be much higher than in the local vicinity.

We experimented with ionization models that allowed for the enhancement of $\Gamma(\mathrm{H\,I})$ by placing the clouds closer to β CMa. For one possible location, at the nearest point to α CMa with its white dwarf companion, the increase in the radiation field is not much: the strength of the radiation from Sirius B (Holberg et al. 1998) reaches a maximum of only 0.4 times that of β CMa as seen near the Sun. However this applies only to fluxes observed at wavelengths above the Lyman limit. If there were substantially less H I and He I between Sirius B and the cloud in front of β CMa, the ionizing fluxes could be larger.

We expect that at a distance of 130 pc from the Sun, a cloud is at the smallest possible distance from ϵ CMa (33 pc) and only 26 pc from β CMa (assuming that the most probable distances between us and the stars derived from Hipparcos are correct). Under this condition, the flux of ϵ CMa is enhanced by a factor of 17, and the flux from β CMa increases by a factor of 36. With the spectral distributions given by Vallerga & Welsh (1995) for ϵ CMa and Aufdenberg et al. (1999) for β CMa (after correction for absorption by the H and He between these stars and the Sun), we find that the enhanced fluxes at this position produce hydrogen neutral fractions of 0.25 and 0.037 for Components C and D. These values are close to what we observed and reported in Sect. 4.2.

To some degree, our results are dependent on the assumed $N(\mathrm{H\,I})$ and $N(\mathrm{He\,I})$ between the ionizing sources and most of the gas in the components. Absorption in front of β CMa is constrained by the column densities that we observed, whereas those for ϵ CMa are arbitrary. For Component C our adopted columns were $N(\mathrm{H\,I}) = 1.1\ 10^{18}\mathrm{cm}^{-2}$ for β CMa and $1.1\ 10^{17}\mathrm{cm}^{-2}$ for ϵ CMa (this low value was required to raise the ionization high enough). For Component D, we made the columns in front of both ϵ CMa and β CMa equal to $N(\mathrm{H\,I}) = 2\ 10^{17}\mathrm{cm}^{-2}$. For both components, we made the He I to H I ratio in the absorbing gas consistent with what we found from the ionization equilibrium calculations.

Our ionization equilibrium calculations indicate that both clouds are located in a region close to ϵ and β CMa where the radiation fields are strongly enhanced. Note also that a physically separate region, perhaps an outer layer of the cloud representing Component D that has evolved to a more fully ionized state, is revealed by the presence of Si III.

The fractional ionization of He that we compute is not very substantial. Singly ionized He accounts for only 6% (Component C) and 19% (Component D) of the total He, even when the material is placed at the position where the radiation fields from ϵ and β CMa are enhanced by the large factors given above. The total column density $N(\mathrm{He\,I})_{\mathrm{C+D}} = 1.6\,10^{18}\mathrm{cm}^{-2}$, which is above the lower limits stated in Sect. 4.2. For Component C, the computed He I/H I of 0.38 agrees with the general results of Wolff et al. (1999), while the much higher ionization of H in Component D produces a considerably larger He I/H I=2.2.

Acknowledgements. The observations reported in this paper are from a guest investigator program that was approved by NASA as a part of the US share of observing time on the ORFEUS-SPAS II flight in 1996, a joint undertaking of the US and German space agencies, NASA and DARA. The successful execution of our observations was the product of efforts over many years by engineering teams at Princeton University Observatory, Ball Aerospace Systems Group (the industrial subcontractor for the IMAPS instrument) and Daimler-Benz Aerospace (the German firm that built the ASTRO-SPAS spacecraft and conducted mission operations). Contributions to the success of IMAPS also came from the generous efforts by many members of the Optics Branch of the NASA Goddard Space Flight Center (grating coatings and testing) and from O. H. W. Siegmund and S. R. Jelinsky at the Berkeley Space Sciences Laboratory (deposition of the photocathode material).

We are grateful to Martin Lemoine for providing his absorption line fitting software that we used to derive the component column densities. This research was supported by NASA grant NAG5−616 to Princeton University.

References

Allan R.J., Clegg R.E.S., Dickinson A.S., Flower D.R., 1988, MNRAS, 235, 1245
Anders E., Grevesse N., 1989, Geochim. Cosmochim. Acta 53, 197
Aufdenberg J.P., Hauschildt P.H., Baron E., 1999, MNRAS, 302, 599
Butler S.E., Dalgarno A., 1979, ApJ 234, 765
Cardelli J.A., Mathis J.S., Ebbets D.C., Savage B.D., 1993, ApJ 402, L17
Cardelli J.A., Meyer D.M., Jura M., Savage B.D., 1996, ApJ 467, 334
Cardelli J.A., Savage B.D., Bruhweiler F.C., et al., 1991a, ApJ 377, L57
Cardelli J.A., Savage B.D., Ebbets D.C., 1991b, ApJ 383, L23
Cassinelli J.P., Cohen D.H., MacFarlane J.J., et al., 1995, ApJ 438, 932
Cassinelli J.P., Cohen D.H., MacFarlane J.J., et al., 1996, ApJ 460, 949
Cheng K.-P., Bruhweiler F.C., 1990, ApJ 364, 573
Cowie L.L., Jenkins E.B., Songaila A., York D.G., 1979, ApJ 232, 467
Dupin O., Gry C., 1998, A&A 335, 661
Field G.B., Steigman G., 1971, ApJ 166, 59
Fitzpatrick E.L., 1996, ApJ 473, L55
Fitzpatrick E.L., 1997, ApJ 482, L199
Fitzpatrick E.L., Spitzer L., 1997, ApJ 475, 623
Gargaud M., McCarroll R., Valiron P., 1982, A&A 106, 197
Gry C., York D.G., Vidal-Madjar A., 1985, ApJ 296, 593
Gry C., Lemonon L., Vidal-Madjar A., Lemoine M., Ferlet R., 1995, A&A 302, 497
Hayes M.A., Nussbaumer H., 1984, A&A 134, 193
Hibbert A., Dufton P.L, Keenan F.P., 1985, MNRAS 213, 721
Holberg J.B., Barstow M.A., Bruhweiler F.C., Cruise A.M., Penny A.J., 1998, ApJ 497, 935
Hurwitz M., Bowyer S., Bristol R., et al., 1998, ApJ 500, L1
Jelinsky P., Vallerga J.V., Edelstein J., 1995, ApJ 442, 653
Jenkins E.B., Joseph C.L., Long D., et al., 1988, in Ultraviolet Technology II, Huffman R.E. (ed.) (Proceedings SPIE, 932.) The International Society for Optical Engineering, Bellingham, 213
Jenkins E.B., Reale M.A., Zucchino P.M., Sofia U.J., 1996, Astr. and Space Sci. 239, 315
Jura M., 1974, ApJ 191, 375
Keenan F.P., Lennon D.J., Johnson C.T., Kingston A.E., 1986, MNRAS 220, 571
Lallement R., Bertin P., 1992, A&A 266, 479
Lallement R., Bertin P., Ferlet R., Vidal-Madjar A., Bertaux J.L., 1994, A&A 286, 898
Lyu C.H., Bruhweiler F.C., 1996, ApJ 459, 216
Mathis J.S., Mezger P.G., Panagia N., 1983, A&A 128, 212
Meyer D.M., Cardelli J.A., Sofia U.J., 1997, ApJ 490, L103
Meyer D.M., Jura M., Cardelli J.A., 1998, ApJ 493, 222
Meyer D.M., Jura M., Hawkins I., Cardelli J.A., 1994, ApJ 437, L59
Morton D.C., 1991, ApjS 77, 119
Nussbaumer H., Storey P.J., 1981, A&A 96, 91
Nussbaumer H., Storey P.J., 1986, A&AS 64, 545
Sarazin C.L., Rybicki G.B., Flannery B.P., 1979, ApJ 230, 456
Savage B.D., Sembach K.R., 1996, ARAA 34, 279
Shull J.M., van Steenberg M., 1982, ApJS 48, 95
Sofia U.J., Cardelli J.A., Guerin K.P., Meyer D.M., 1997, ApJ 482, L105
Sofia U.J., Fitzpatrick E.L., Meyer D.M., 1998, ApJ 504, L47
Sofia U.J., Jenkins E.B., 1998, ApJ 499, 951
Spitzer L., 1978, *Physical Processes in the Interstellar Medium*, (New York, Wiley-Interscience)
Vallerga J.V., 1997, ApJ 497, 921
Vallerga J.V., Welsh B.Y., 1995, ApJ 444, 702
Verner D.A., Ferland G.J., Korista K.T., Yakovlev D.G., 1996, ApJ 465, 487
Wolff B., Koester D., Lallement R., 1999, A&A 346, 969